Effective bandstructure in the insulating phase versus strong dynamical correlations in metallic VO_2

Jan M. Tomczak,[1,2] Ferdi Aryasetiawan,[2] and Silke Biermann[1]
[1]*Centre de Physique Théorique, Ecole Polytechnique, CNRS, 91128 Palaiseau Cedex, France*
[2]*Research Institute for Computational Sciences, AIST, Umezono 1-1-1, Tsukuba Central 2, Tsukuba Ibaraki 305-8568, Japan*
(Received 3 July 2008; published 3 September 2008)

Using a general analytical continuation scheme for cluster dynamical mean-field calculations, we analyze real-frequency self-energies, momentum-resolved spectral functions, and one-particle excitations of the metallic and insulating phases of VO_2. While for the former dynamical correlations and lifetime effects prevent a description in terms of quasiparticles, the excitations of the latter allow for an effective bandstructure. We construct an orbital dependent, but static one-particle potential that reproduces the essentials of the full many-body spectrum. Yet, the ground state is well beyond a static one-particle description. The emerging picture gives a nontrivial answer to the decade-old question of the nature of the insulator, which we characterize as a "many-body Peierls" state, stressing the joint effect of lattice symmetry breaking and Coulomb correlations.

DOI: 10.1103/PhysRevB.78.115103 PACS number(s): 71.27.+a, 71.15.Mb, 71.30.+h, 79.60.−i

I. INTRODUCTION

Describing electronic correlations is a challenge for modern condensed-matter physics. While weak correlations slightly modify quasiparticle states, by broadening them with lifetime effects and shifting their energies, strong enough correlations can entirely invalidate the band picture by inducing a Mott insulating state.

In a half-filled one-band model, an insulator is realized above a critical ratio of interaction to bandwidth. Though more complex scenarios exist in realistic multiband cases, a common feature of compounds that undergo a metal-insulator transition (MIT) upon the change of an external parameter, such as temperature or pressure, is that the respective insulator feels stronger correlations than the metal, since it is precisely their enhancement that drives the system insulating.

In this paper we discuss a material where this rule of thumb is inverted: We argue that in VO_2 it is the insulator that is less correlated, in the sense that bandlike excitations are better defined and have longer lifetimes than in the metal. Albeit, *neither* phase is well described by standard bandstructure techniques. Using an analytical continuation scheme for quantum Monte Carlo solutions to dynamical mean field theory (DMFT),[1,2] we discuss quasiparticle lifetimes, **k**-resolved spectra (for comparison with future angle-resolved photoemission experiments) and effective bandstructures. While dynamical effects are crucial in the metal, the excitations of the insulator are well described within a static picture; for the insulator we devise an effective one-particle potential that captures the interacting excitation spectrum. Still, the corresponding ground state is far from a Slater determinant, leading us to introduce the concept of a "many-body Peierls" insulator.

The MIT of VO_2 has intrigued solid-state physicists for decades.[3–18] A high-temperature metallic rutile (R) phase transforms at $T_c=340$ K into an insulating monoclinic structure (M1), in which vanadium atoms pair up to form tilted dimers along the c axis. The resistivity jumps up by two orders of magnitude, yet no local moments form. Despite extensive efforts, the mechanism of the transition is still under debate.[5,11,14–18] Two scenarios compete: In the Peierls picture the structural aspect (unit-cell doubling) causes the MIT, while in the Mott picture local correlations predominate.

VO_2 has a d^1 configuration and the crystal field splits the $3d$ manifold into t_{2g} and empty e_g^σ components. The former further split into e_g^π and a_{1g} orbitals, which overlap in R-VO_2, accounting for the metallic character. Still, the quasiparticle peak seen in photoemission (PES) (Refs. 15–17) is much narrower than the Kohn-Sham spectrum of density-functional theory (DFT) in the local-density approximation (LDA),[11] and eminent satellite features evidenced in PES are absent. In M1-VO_2, the a_{1g} form bonding/antibonding orbitals, due to the dimerization. As discussed by Goodenough,[4] this also pushes up the e_g^π relative to the a_{1g}. Yet, the LDA yields a metal.[11] Nonlocal correlations beyond LDA were shown to be essential.[19–21] Indeed, recent Cluster DMFT (CDMFT) calculations,[19] in which a two-site vanadium dimer constituted the DMFT impurity, opened a gap, agreeing well with PES and x-ray experiments.[15–18,22–25]

II. METHODS AND RESULTS

Starting from these LDA+CDMFT results[19] for the Matsubara t_{2g} Green's function $G(\imath\omega_n)$ we deduce the real-frequency Green's function $G(\omega)$ by the maximum entropy method[26] and a Kramers-Kronig transform. The self-energy matrix $\Sigma(\omega)$ we obtain by numerical inversion of $G(\omega)=\Sigma_k[\omega+\mu-H_k-\Sigma(\omega)]^{-1}$,[1,2] with the LDA Hamiltonian H, and the chemical potential μ.

A. Rutile VO_2

Figure 1 shows (a) the diagonal elements of the R-VO_2 self-energy, and (b) the resulting **k**-resolved spectrum. Notwithstanding minor details, the a_{1g} and e_g^π self-energies exhibit a similar *dynamical* behavior. The real parts at zero energy, $\Re\Sigma(0)$, entailing relative shifts of quasiparticle bands, are almost equal, congruent with the low changes in

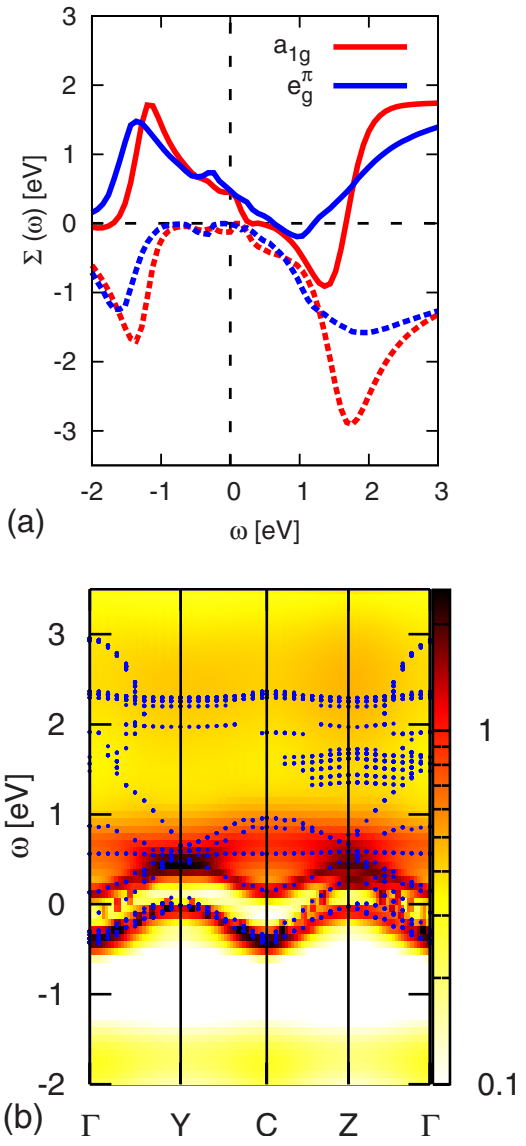

FIG. 1. (Color online) Rutile VO_2: (a) self-energy ($\Sigma-\mu$). Real (imaginary) parts are solid (dashed). (b) spectral function $A(\mathbf{k},\omega)$ and solutions of the QPE (blue). The LHB is the (yellow) region at −1.7 eV, the broad upper Hubbard band appears (yellow) at ~2.5 eV.

their occupations vis-à-vis LDA,[19] and with the isotropy evidenced in experiment.[27]

Neglecting lifetime effects (i.e., $\Im\Sigma\approx 0$), one-particle excitations are given by the poles $\omega_{\mathbf{k}}$ of $G(\omega)$: $\det[\omega_{\mathbf{k}}+\mu-H_{\mathbf{k}}-\Re\Sigma(\omega_{\mathbf{k}})]=0$. We shall refer to this as the quasiparticle equation (QPE).[28] For static or absent $\Re\Sigma$ this reduces to a simple eigenvalue problem. In regions of low imaginary parts of the self-energy, $\Im\Sigma$, the QPE solutions will give an accurate description of the position of spectral weight and constitute an effective bandstructure of the interacting system. Yet, due to the frequency dependence, the number of solutions is no longer bounded to the number of orbitals and satellite structures may induce additional poles in Green's function.

Below (above) −0.5 (0.2) eV, the imaginary parts of the self-energy—the inverse lifetime—of R-VO_2 is considerable. Due to our limited precision for $\Im\Sigma(0)$, we have not attempted a temperature dependent study to assess the experimentally found bad metal behavior, but the resistivity exceeding the Ioffe-Regel-Mott limit[29] indicates that even close to the Fermi level, coherence is not fully reached. At low energy, the QPE solutions [dots in Fig. 1(b)] closely follow the spectral weight. Above 0.2 eV, regions of high intensity appear, howbeit, the larger $\Im\Sigma$ broadens the excitations, and no coherent features emerge, though the positions of some e_g^π derived excitations are discernible. At high energies, both positive and negative, distinctive features appear in $\Im\Sigma(\omega)$ that are responsible for lower (upper) Hubbard bands, seen in the spectrum at around −1.7 (2.5) eV. The upper Hubbard band exhibits a pole structure that reminds of the low-energy quasiparticle bandstructure, which is in line with observations that quasiparticle dispersions are generally reflected in the dispersion of the Hubbard bands.[30] Hence, an effective band picture is limited to the close vicinity of the Fermi level, and R-VO_2 has to be considered as a strongly correlated metal (the weight of the quasiparticle peak is of the order of 0.6). This is experimentally corroborated by the fact that an increase in the lattice spacing by Nb-doping results in a Mott insulator of rutile structure.[7]

B. Monoclinic VO_2

1. The self-energy and its implications

The imaginary parts of the M1 a_{1g} on site, and $a_{1g}-a_{1g}$ intradimer self-energies, Fig. 2(a), strongly depend on frequency and are larger than any element in R-VO_2, usually a hallmark of increased correlations. However, we shall argue that correlations are in fact weaker than in the metal. Indeed, the dimerization in M1 leads to strong intersite fluctuations, evidenced by the significant intradimer $a_{1g}-a_{1g}$ self-energy. Figure 3 displays the M1-VO_2 self-energy in the a_{1g} bonding/antibonding (b,ab) basis, $\Sigma_{b/ab}=\Sigma_{a_{1g}}\pm\Sigma_{a_{1g}-a_{1g}}$ The a_{1g} (anti)bonding imaginary part is low and varies little with frequency in the (un)occupied part of the spectrum, thus allowing for coherent weight. In the opposite regions, the imaginary parts reach huge values. The e_g^π elements are flat, and their imaginary parts tiny. This is a direct consequence of the drastically reduced e_g^π occupancy which drops to merely 0.14. These almost empty orbitals feel only weak correlations, and sharp bands are expected at all energies. A first idea for the a_{1g} excitations is obtained from the intersections $\omega+\mu-\epsilon_{b/ab}(\mathbf{k})=\Re\Sigma_{b/ab}(\omega)$ as depicted in Fig. 3(a), where the black stripes delimit the LDA a_{1g} bandwidths. The (anti)bonding band appears as the crossing of the (blue) red solid line with the stripe at (positive) negative energy. Hence, the (anti)bonding band emerges at (2.5) −0.75 eV. Still, the antibonding band is much broadened since $\Im\Sigma_{ab}$ reaches −1 eV.

2. Momentum-resolved spectral functions

To confirm the above analysis, we solved the QPE and calculated the **k**-resolved spectrum [Fig. 4(a)]. As expected, reasonably coherent weight appears over nearly the *entire* spectrum from −1 to +2 eV, whose position coincides with

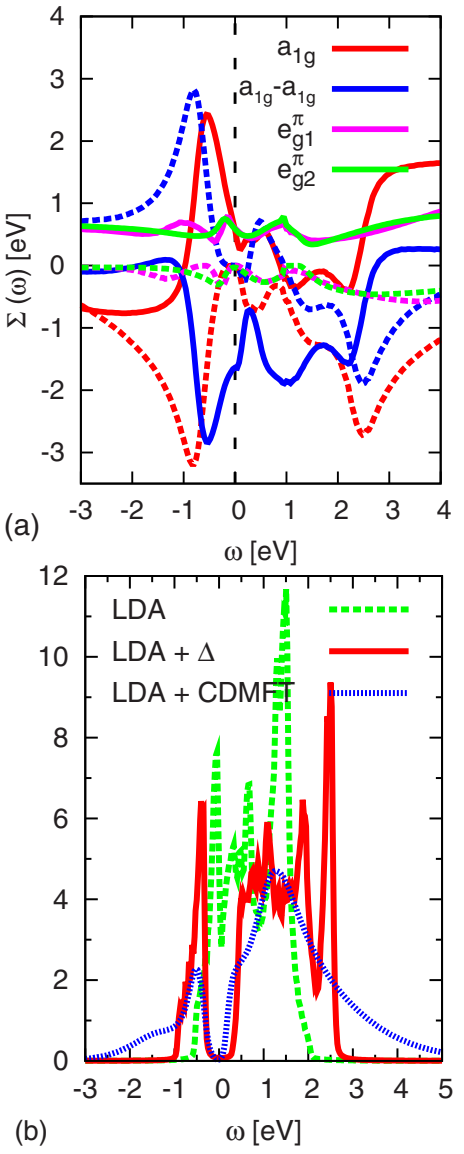

FIG. 2. (Color online) Monoclinic VO_2: (a) Self-energy ($\Sigma-\mu$), real (imaginary) parts are solid (dashed). (b) Comparison of the LDA DOS with the LDA+CDMFT spectrum and the DOS when applying the static potential Δ. See text for discussion.

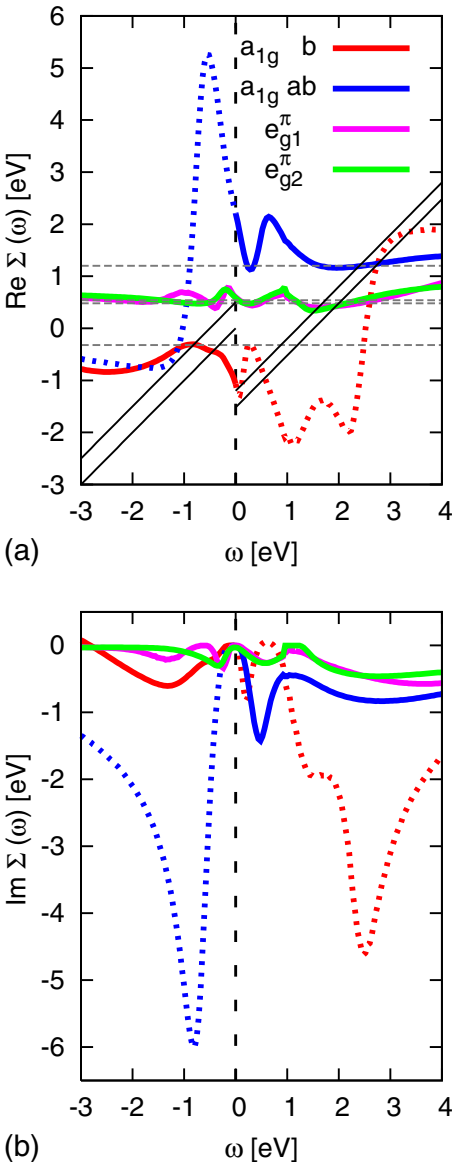

FIG. 3. (Color online) Self-energy ($\Sigma-\mu$) of M1-VO_2 in the a_{1g} bonding/antibonding basis: (a) real parts. The black stripes delimit the a_{1g} LDA bandwidths, dashed horizontal lines indicate the values of the static potential Δ. (b) imaginary parts. Self-energy elements are dotted in regions irrelevant for the spectrum.

the QPE poles: The filled bands correspond to the a_{1g} bonding orbitals, while above the gap, the e_g^π bands give rise to sharp features. The antibonding a_{1g} is not clearly distinguished since e_g^π weight prevails in this range. The satellites have faded; a mere shoulder at −1.5 eV reminds of the lower Hubbard band.

3. Construction of an effective one-particle potential

Contrary to R-VO_2, the number of solutions to the quasiparticle equation equals the orbital dimension. Since, moreover, the real parts of the M1-VO_2 self-energy are almost constant for relevant energies,[31] we construct a static potential, Δ, by evaluating the dynamical self-energy at the LDA band centers (pole energies) for the e_g^π (a_{1g}), see Fig. 3(a).[32] Figure 4(b) shows the bandstructure of $H_{\mathbf{k}}+\Delta$: The agreement with the DMFT poles is excellent. We further calculate the density of states (DOS) corresponding to the bandstructure of $H_{\mathbf{k}}+\Delta$. This quantity, displayed in Fig. 2(b), thus takes into account the shifts of the bands, but not their life-times. The charge gap is correctly opened and the position of spectral weight agrees well with the LDA+CDMFT spectral function. Yet the missing information on life-time effects, which are small but finite, causes excitations to be too sharply defined. Our one-particle potential, albeit static, depends on the orbital, and is thus nonlocal. We emphasize the conceptual difference to the Kohn-Sham (KS) potential of DFT; the latter generates an effective one-particle problem with the ground-state density of the true system. The KS energies and states are *auxiliary* quantities. Our one-particle potential, Δ, on the contrary, was designed to reproduce the excitation spectrum of the interacting system. The eigenval-

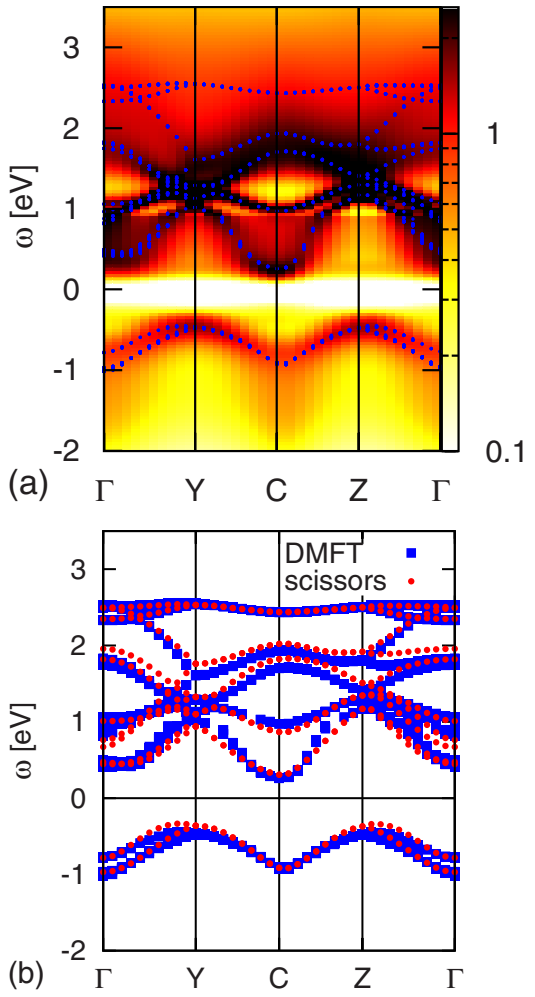

FIG. 4. (Color online) M1-VO_2: (a) spectral function $A(\mathbf{k},\omega)$. (blue) dots [(a) & (b)] are solutions of the QPE. (b) The (red) dots are the eigenvalues of $H_{\mathbf{k}}+\Delta$. See text for discussion.

ues of $H_{\mathbf{k}}+\Delta$ are thus *not* artificial. Still, like in DFT, the eigenstates are Slater determinants by construction, although the true states are not. The crucial point for M1-VO_2 is that *spectral properties* are capturable with this effective one-particle description. It is in this sense that M1-VO_2 exhibits only weak correlation effects. The weight of the bonding excitation is $Z=[1-\partial_\omega \Re\Sigma_b(\omega)]^{-1}_{\omega=-0.7\ \mathrm{eV}} \approx 0.75$, and thus larger than the rutile quasiparticle weight (see above).

C. Elucidating the coherence of M1 VO_2

1. Model considerations

What is at the origin of this overall surprising coherence? For the e_g^π orbitals, this simply owes to their depletion. For the nearly half-filled a_{1g} orbitals the situation is more intricate. It is a joint effect of charge transfer into the a_{1g} bands, and the bonding/antibonding splitting. Indeed, the filled bonding band experiences only weak fluctuations, due to its separation of several eV from the antibonding one. To substantiate these qualitative arguments, we resort to the following model, which treats the solid as a collection of Hubbard dimers:

$$H = -t\sum_{l\sigma}(c^\dagger_{l1\sigma}c_{l2\sigma}+h.c.) - t_\perp \sum_{\substack{i=1,2\\ \langle l,l'\rangle}} c^\dagger_{li\sigma}c_{l'i\sigma} + U\sum_{il} n_{li\uparrow}n_{li\downarrow}. \tag{1}$$

Here, $c^\dagger_{li\sigma}$ ($c_{li\sigma}$) creates (destroys) an electron with spin σ on site i of the lth dimer. t is the intradimer, $t_\perp$ the interdimer hopping, U the on-site Coulomb repulsion, and we assume half-filling. First, we discuss the $t_\perp \to 0$ limit, which is an isolated dimer; the Hubbard molecule.

2. The Hubbard molecule

We choose $t=0.7$ eV, the LDA intradimer $a_{1g}-a_{1g}$ hopping, and $U=4.0$ eV (Ref. 19) for all evaluations. The bonding/antibonding splitting, $\Delta_{bab}=-2t+\sqrt{16t^2+U^2}=3.48$ eV, gets *enhanced* with respect to the $U=0$ case. In M1-VO_2, the embedding into the solid, and the hybridization with the e_g^π reduce the splitting to ~ 3 eV, as can be inferred from the one-particle poles (Fig. 4), consistent with experiment.[15] The ground state of the dimer is given by[33] $|\psi_0\rangle=\{4t/(c-U)(|\downarrow\uparrow\rangle-|\uparrow\downarrow\rangle)+(|\uparrow\downarrow 0\rangle+|0\uparrow\downarrow\rangle)\}/a$ which is intermediate to the Slater determinant (SD) (the four states having equal weight), and the Heitler-London (HL) limit (double occupancies projected out). With the VO_2 parameters, the model dimer is close to the Heitler-London limit.[6] The inset of Fig. 5(b) shows the projections of the ground state onto the Slater determinant and the Heitler-London state. The former, $|\langle SD|\psi_0\rangle|^2$, equals the weight of the band-derived features in the spectrum (for $U>0$ satellites appear), while the other measures the double occupancy $\Sigma_i\langle n_{i\uparrow}n_{i\downarrow}\rangle = 1-|\langle HL|\psi_0\rangle|^2$. For $U=4.0$ eV the latter is largely suppressed, as a consequence of the interaction: The N-particle state is clearly not a Slater determinant. Still, the overlap with the Slater determinant, and thus the coherent weight, remains significant, i.e., one-particle excitations survive and lifetimes are large. To do justice to the seemingly opposing tendencies of correlation driven non-Slater-determinant behavior, coexisting with a bandlike spectrum, we introduce the notion of a many-body Peierls state.

The charge transfer from the e_g^π into the then almost half-filled a_{1g} orbitals, finds its origin in the effective reduction of the local interaction in the bonding/antibonding configuration. While for $U=4$ eV, $\langle SD|H|SD\rangle=2.0$ eV in the Slater determinant limit, it reduces to merely $\langle\psi_0|H|\psi_0\rangle=0.91$ eV in the ground state. In fact, intersite fluctuations are an efficient way to avoid the on-site Coulomb repulsion. In M1-VO_2, this effect manifests itself in a close cancellation of the local and intersite self-energies in the (un)occupied parts of the spectrum for the (anti)bonding a_{1g} orbitals.

The gap opening in VO_2 thus owes to two effects: The self-energy enhancement of the a_{1g} bonding/antibonding splitting, and a charge transfer from the e_g^π orbitals. The difference in $\Re\Sigma$ corresponds to this depopulation, seen in experiments[27] and theoretical studies,[14,19] and leads to the separation of the a_{1g} and e_g^π at the Fermi level. *The local interactions thus amplify Goodenough's scenario.*

3. A solid of Hubbard dimers

Does the embedding of the dimer into the solid qualitatively alter our picture of the M1 phase? The model, Eq. (1),

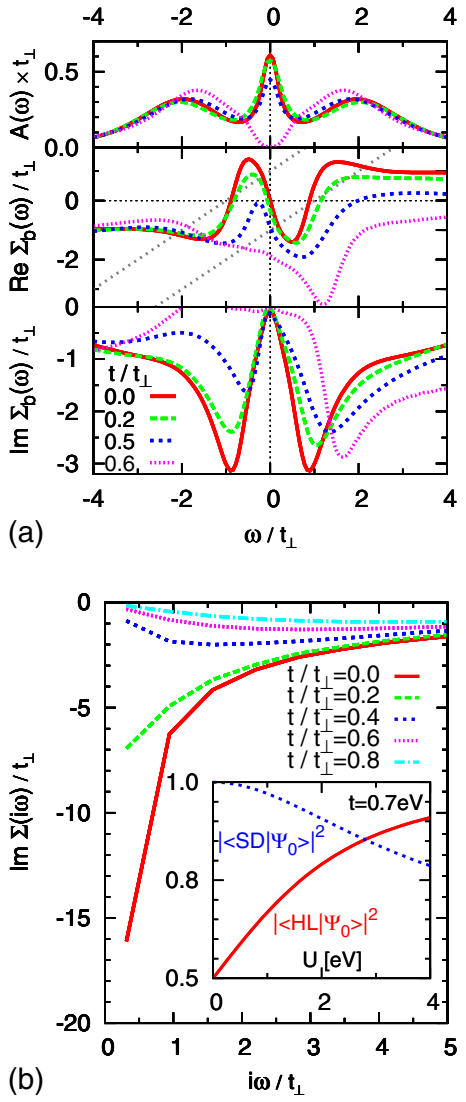

FIG. 5. (Color online) (a) spectral function (top), real (middle), imaginary (bottom) *bonding* self-energy Σ_b of the CDMFT solution to Eq. (1) for $U=4.0t_\perp$, $\beta=10/t_\perp$, and varying intradimer hopping $t/t_\perp$. $\Re\Sigma_b(\omega)=-\Re\Sigma_{ab}(-\omega)$, $\Im\Sigma_b(\omega)=\Im\Sigma_{ab}(-\omega)$ by symmetry. Dashed gray lines indicate the graphical QPE construction. (b) Imaginary Matsubara self-energy, $\Im\Sigma_b(\imath\omega)=\Im\Sigma_{ab}(\imath\omega)$, for $U=6t_\perp$, $\beta=10/t_\perp$ and varying t. Inset: Projection of the Slater determinant and Heitler London limit on the Hubbard molecule ground state ($t=0.7$ eV, $t_\perp=0$) vs U.

has been studied within CDMFT in Ref. 34, establishing a rich phase diagram with a metal, Mott- and band-insulator phase. Here, we argue that the above interpretation survives the branching of the interdimer hopping. Moreover, we study the essentials of the rutile to M1 MIT by scanning through the degree of dimerization t at constant interaction strength U and embedding, or interdimer hopping, $t_\perp$. For the latter we assume a semicircular density of states $D_\perp(\omega)$ of bandwidth $W=4t_\perp$. In M1-VO_2, the $t_\perp$ for direct a_{1g}-a_{1g} hopping is rather small, yet e_g^π hybridizations lead to an effective $D_\perp$ bandwidth of about 1 eV. We choose $U=4t_\perp$, and an inverse temperature $\beta=10/t_\perp$. Figure 5(a) displays the orbital traced local spectral function $A(\omega)=A_b(\omega)+A_{ab}(\omega)$ (b,ab denoting again the bonding/antibonding combinations. See also Fig. 3 in Ref. 34) and the bonding self-energy $\Sigma_b(\omega)$ for different intradimer hoppings t: In the absence of t, the result equals by construction the single-site DMFT solution ($\Sigma_b=\Sigma_{ab}$), which, for our parameters, is a correlated metal, analog to R-VO_2. The spectral weight at the Fermi level is given by $A_{b/ab}(0)=D_\perp[\pm t-\Re\Sigma_{b/ab}(0)]$, with $\Re\Sigma_{b/ab}(0)=\mp\Re\Sigma_{ab}(0)$. Thus a MIT occurs at $t+\Re\Sigma_{ab}(0)=2t_\perp$, when all spectral weight has been shifted out of the bandwidth. Above $t/t_\perp=0.5$ we find a many-body Peierls phase corresponding to M1-VO_2. In Fig. 5(a) we have indicated again the graphical QPE approach; the system evolves from three solutions *per orbital* (Kondo resonance, lower and upper Hubbard band) at $t=0$ to a single one at $t/t_\perp=0.6$. Hence the peaks in the insulator are *not* Hubbard satellites, but just shifted bands. The embedding, $t_\perp$, broadens the excitations and washes out the satellites of the isolated dimer, like for M1-VO_2. Still, as a function of t, the coherence of the spectrum increases, since the imaginary part of the (anti)bonding self-energy subsides at the renormalized (anti)bonding excitation energies. Our model thus captures the essence of the rutile to M1 transition, reproducing both, the dimerization induced increase in coherence, and the shifting of excitations.

D. Addenda: The M2 phase

Under uniaxial pressure or Cr doping, VO_2 develops the insulating M2 phase[7–9] in which every second vanadium chain along the c axis consists of untilted dimers, whereas in the others only the tilting occurs. We may now speculate that the dimerized pairs in M2 form a_{1g} Peierls singlets as in M1, while the tilted pairs are in a Mott state. Hence, we interpret the seminal work of Pouget and coworkers[7–9] as the observation of a Mott to many-body Peierls transition taking place on the tilted chains when going from M2 to M1. To illustrate this, we solve again Eq. (1) for appropriate parameters. The tilted M2 chains are akin to the rutile phase, yet with a reduced a_{1g} bandwidth.[11] Thus we now choose $U=6t_\perp$, $\beta=10/t_\perp$, and vary t. All solutions shown in Fig. 5(b) are insulating, however, the diverging self-energy at vanishing intradimer coupling ($t=0$, tilted "M2" chains) becomes regularized with the bond enhancement ($t>0$, "M1"). The imaginary part of the self-energy gets flatter and the system thus more coherent. The above is consistent with the finding of (S=0)S=1/2 for the (dimerized) tilted pairs in M2-VO_2.[7–9]

III. CONCLUSIONS

While our results do not exclude surprises in the direct vicinity of T_c,[35] the nature of insulating VO_2 is shown to be rather "bandlike" in the above sense. Our analytical continuation scheme allowed us to *explicitly calculate* this bandstructure. The latter can also be derived from a static one-particle potential. Yet, this does *not* imply a one-particle picture for quantities other than the spectrum. Above all, the ground state is not a Slater determinant. Hence, we qualify M1-VO_2 as a many-body Peierls phase. We argue that the weakness of lifetime effects results from strong intersite fluctuations that circumvent local interactions in an otherwise

strongly correlated solid. This is in striking contrast to the strong dynamical correlations in the metal, which is dominated by important lifetime effects and incoherent features.

ACKNOWLEDGMENTS

We thank H. T. Kim, J. P. Pouget, M. M. Qazilbash, and A. Tanaka for valuable discussions and A. I. Poteryaev, A. Georges, and A. I. Lichtenstein for discussions and the collaboration[19] that was our starting point. We thank AIST, Tsukuba, for hospitality. J.M.T. was supported by JSPS. This work was further supported by the French ANR under project CORRELMAT. Computer time was provided by IDRIS, Orsay (Project No. 071393).

[1] Jan M. Tomczak, Ph.D. thesis, Ecole Polytechnique, 2007.
[2] J. M. Tomczak and S. Biermann, J. Phys.: Condens. Matter **19**, 365206 (2007).
[3] A. Zylbersztejn and N. F. Mott, Phys. Rev. B **11**, 4383 (1975).
[4] J. B. Goodenough, J. Solid State Chem. **3**, 490 (1971).
[5] R. M. Wentzcovitch, W. W. Schulz, and P. B. Allen, Phys. Rev. Lett. **72**, 3389 (1994).
[6] C. Sommers and S. Doniach, Solid State Commun. **28**, 133 (1978).
[7] J. P. Pouget and H. Launois, J. Phys. (Paris) **37**, C4 (1976).
[8] J. P. Pouget, H. Launois, J. P. D'Haenens, P. Merenda, and T. M. Rice, Phys. Rev. Lett. **35**, 873 (1975).
[9] J. P. Pouget, H. Launois, T. M. Rice, P. Dernier, A. Gossard, G. Villeneuve, and P. Hagenmuller, Phys. Rev. B **10**, 1801 (1974).
[10] A. Continenza, S. Massidda, and M. Posternak, Phys. Rev. B **60**, 15699 (1999).
[11] V. Eyert, Ann. Phys. **11**, 650 (2002).
[12] L. N. Bulaevskii and D. I. Khomskii, Sov. Phys. Solid State **9**, 2422 (1968).
[13] M. A. Korotin, N. A. Skorikov, and V. I. Anisimov, Phys. Met. Metallogr. **94**, 17 (2002).
[14] A. Tanaka, J. Phys. Soc. Jpn. **72**, 2433 (2003).
[15] T. C. Koethe, Z. Hu, M. W. Haverkort, C. Schussler-Langeheine, F. Venturini, N. B. Brookes, O. Tjernberg, W. Reichelt, H. H. Hsieh, H.-J. Lin, C. T. Chen, and L. H. Tjeng, Phys. Rev. Lett. **97**, 116402 (2006).
[16] R. Eguchi, M. Taguchi, M. Matsunami, K. Horiba, K. Yamamoto, Y. Ishida, A. Chainani, Y. Takata, M. Yabashi, D. Miwa, Y. Nishino, K. Tamasaku, T. Ishikawa, Y. Senba, H. Ohashi, Y. Muraoka, Z. Hiroi, and S. Shin, Phys. Rev. B **78**, 075115 (2008).
[17] S. Shin, S. Suga, M. Taniguchi, M. Fujisawa, H. Kanzaki, A. Fujimori, H. Daimon, Y. Ueda, K. Kosuge, and S. Kachi, Phys. Rev. B **41**, 4993 (1990).
[18] G. A. Sawatzky and D. Post, Phys. Rev. B **20**, 1546 (1979).
[19] S. Biermann, A. Poteryaev, A. I. Lichtenstein, and A. Georges, Phys. Rev. Lett. **94**, 026404 (2005).
[20] A. Liebsch, H. Ishida, and G. Bihlmayer, Phys. Rev. B **71**, 085109 (2005).
[21] M. S. Laad, L. Craco, and E. Müller-Hartmann, Phys. Rev. B **73**, 195120 (2006).
[22] E. Goering, M. Schramme, O. Müller, R. Barth, H. Paulin, M. Klemm, M. L. denBoer, and S. Horn, Phys. Rev. B **55**, 4225 (1997).
[23] E. Z. Kurmaev, V. M. Cherkashenko, Yu M. Yarmoshenko, St Bartkowski, A. V. Postnikov, M. Neumann, L. C. Duda, J. H. Guo, J. Nordgren, V. A. Perelyaev, and W. Reichelt. J. Phys.: Condens. Matter **10**, 4081 (1998).
[24] K. Okazaki, H. Wadati, A. Fujimori, M. Onoda, Y. Muraoka, and Z. Hiroi, Phys. Rev. B **69**, 165104 (2004).
[25] M. Abbate, F. M. F. de Groot, J. C. Fuggle, Y. J. Ma, C. T. Chen, F. Sette, A. Fujimori, Y. Ueda, and K. Kosuge, Phys. Rev. B **43**, 7263 (1991).
[26] M. Jarrell and J. E. Gubernatis, Phys. Rep. **269**, 133 (1996).
[27] M. W. Haverkort, Z. Hu, A. Tanaka, W. Reichelt, S. V. Streltsov, M. A. Korotin, V. I. Anisimov, H. H. Hsieh, H.-J. Lin, C. T. Chen, D. I. Khomskii, and L. H. Tjeng, Phys. Rev. Lett. **95**, 196404 (2005).
[28] We solve the equation numerically by iterating until self-consistency within an accuracy of 0.05 eV.
[29] M. M. Qazilbash, K. S. Burch, D. Whisler, D. Shrekenhamer, B. G. Chae, H. T. Kim, and D. N. Basov, Phys. Rev. B **74**, 205118 (2006).
[30] J. Hubbard, Philos. Trans. R. Soc. London, Ser. A **276**, 238 (1963).
[31] Explaining why LDA+U opens a gap (Refs. 13 and 20), yet while missing the correct bonding/antibondingsplitting.
[32] $\Delta_{e^{\pi}_{g1}}=0.48$ eV, $\Delta_{e^{\pi}_{g2}}=0.54$ eV, $\Delta_b=-0.32$ eV, $\Delta_{ab}=1.2$ eV.
[33] $a=\sqrt{2(16t^2/(c-U)^2+1)}$, $c=\sqrt{16t^2+U^2}$.
[34] Andreas Fuhrmann, David Heilmann, and Hartmut Monien, Phys. Rev. B **73**, 245118 (2006).
[35] Hyun-Tak Kim, Yong Wook Lee, Bong-Jun Kim, Byung-Gyu Chae, Sun Jin Yun, Kwang-Yong Kang, Kang-Jeon Han, Ki-Ju Yee, and Yong-Sik Lim, Phys. Rev. Lett. **97**, 266401 (2006).